

# Improvement of the Yield during Crystal Growth of SiC by PVT by Proper Selection and Design of Hot Zone Isolation Components

Sven STRÜBER<sup>1,a</sup>, Jonas IHLE<sup>1,b</sup>, Julian ZÖCKLEIN<sup>1,c</sup>,  
Johannes STEINER<sup>1,d</sup>, Peter J. WELLMANN<sup>1,e\*</sup>

<sup>1</sup>Crystal Growth Lab, Materials Department 6, University of Erlangen-Nürnberg (FAU),  
Martensstr. 7, 91058 Erlangen, Germany

<sup>a</sup>sven.strueber@fau.de, <sup>b</sup>jonas.ihle@fau.de, <sup>c</sup>julian.zoecklein@fau.de,  
<sup>d</sup>johannes.steiner@fau.de, <sup>e</sup>peter.wellmann@fau.de

\*Corresponding author

**Keywords:** Bulk growth, Physical vapor transport, PVT, Yield.

**Abstract.** This work discusses three aspects of the PVT growth process to reach a higher SiC crystal yield: (i) Type of carbon isolation material and procedure to maintain reproducible growth conditions from one process to the next. (ii) The pros and cons of temperature and power control (or a mixture of both) during the SiC crystal growth phase of the PVT process; and (iii) the selection of a set of process parameters and the specifications of the grown SiC crystal, which serve as a fingerprint of reproducible growth conditions (related to the selection and design of hot zone isolation components).

## Introduction

The bulk growth process of SiC using the physical vapor transport (PVT) method may be called mature [1-3]. A single-crystalline diameter of 150 mm is state of the art, while a crystal diameter of 200 mm is being promoted as the new standard. Major R&D efforts focus on reducing the dislocation density even further. In this context, improving the yield of the PVT process is a key task. In this paper, we discuss the role of carbon isolation, a key element in achieving the desired growth temperature at a given heating power. To ensure consistent growth conditions throughout the process, which typically takes over 10 days, we discuss the pros and cons of power- or temperature-based process control. Finally, we suggest a procedure to classify reproducible growth processes. Please note that other sources of process instability, such as graphite quality, carbon crucible quality, and SiC seed quality and mounting, are not addressed in this work.

## Experiments

In our study, we analyzed forty 150 mm PVT growth processes, all of which used the same fundamental hot-zone design. Two minor design variations were conducted: cooling channels A and B and crucible variants related to seed mounting #1 and #2 (Fig. 1). Compared to an industrial standard growth process, the number of crystals analyzed is rather low. Nevertheless, the study yields clear recommendations for increasing process reproducibility and yield related to the challenging isolation components of the hot zone.

**PVT Furnace.** The study was carried out using the 150 mm PVT furnace “Sicma 3” provided by the company PVA Crystal Growing Systems GmbH (Wettenberg, Germany), and installed in the crystal growth lab at FAU.

**Hot-Zone Design.** The basic SiC PVT-technology developed in the crystal growth lab at FAU over the last 15 years makes use of the hotzone design I which is highly scalable for crystal diameters from 100 to 150 mm and even 200 mm. In addition, it is hardly sensitive to the heating geometry (shape of induction coil or arrangement of resistive heaters). As a result, the hotzone may be used in many different PVT furnaces with no or only small adaptation. As a previous example, in [4] we have shown, that 100 mm SiC boules can be grown in two different PVT furnaces, i.e. water cooled (FAU

PVT machine) and air cooled (Sicma 3 PVT system from PVA Crystal Growing Systems GmbH) growth chamber, without any adaptation (Fig. 2). The hotzone design developed at FAU aims to serve crystal growth industries with a basic starting growth technology. A SiC crystal recently grown for the presented study is depicted in Fig 3. The fact that the crystalline R&D quality falls behind the industrial standard is related to the lab mission where usually special growth runs stand in the foreground compared to optimization of one special setting. Best areas ( $20 \times 20 \text{ mm}^2$ ) in the 150mm SiC boules presented in this study are MPs =  $0 \text{ cm}^{-2}$ , TSDs =  $570 \text{ cm}^{-2}$  TEDs  $\approx 5970 \text{ cm}^{-2}$  and BPDs  $\approx 9150 \text{ cm}^{-2}$ , respectively.

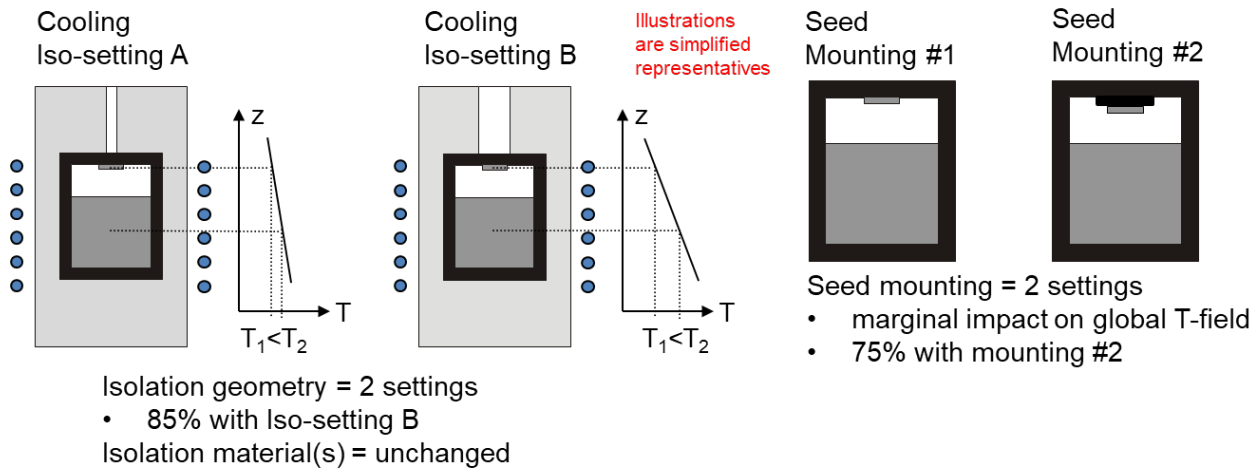


**Fig. 1.** Sketch of the hot zone design variations used within the presented study.

FAU PVT furnace

PVA PVT furnace

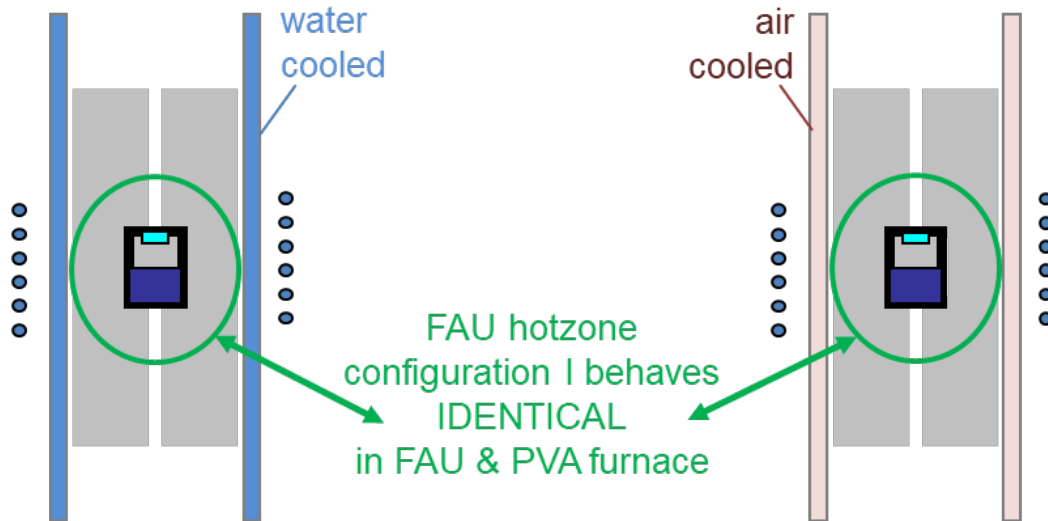


**Fig. 2.** The basic hotzone design I designed by FAU is compatible with different PVT furnace designs like the Sicma series of the company PVA Crystal Growing Systems GmbH.



**Fig. 3.** Example of the side-view of an as-grown 150 mm 4H-SiC (grown using basic hotzone configuration I, cooling channel B and crucible variant #2).

**PVT Process Control.** Computer simulation of the temperature field and optionally also of the mass transport and/or resulting stress in the grown crystal, is an essential standard tool in SiC PVT-growth. For some original publications see [5-10]. The growth process at temperatures above 2000°C in a closed graphite crucible allows only limited sensory access to the physical conditions inside the growth cell. Despite the fundamental hot zone design, the PVT growth process is usually controlled only by setting of the heating power and inert-gas pressure. By measurement of the temperatures at the crucible top and bottom using optical pyrometers, feedback is given to control the progress of the growth process. In principle, X-ray in-situ visualization methods in 2D and 3D [11-13] have been demonstrated since many years, but only few growth facilities are using these advanced methods.

**T-Field Calculation.** Computer simulation has proved to give valuable insight into the growth conditions in front of the crystal growth interface. However, the reliability and technical applicability of the temperature field and mass transport calculations strongly depend on the proper knowledge of the temperature dependent materials data like the temperature dependent heat conductivity, the coefficient of thermal expansion and the electrical conductivity (in case of inductive heating), to name a few important parameters. Often those values are not known from the material provider data sheets. Therefore, we have conducted intense investigations of the thermal properties of carbon materials in the growth temperature regime which have been published in [4, 14, 15].

In addition, also the heat conductivity of the source material has been studied using advanced physical models [4, 16]. It turned out for practical reasons that the source material may be treated quite precisely using a two-zone model where the condensed and partially sintered SiC source may be treated as a porous media (pore size =  $d_{pore}$ ) using Eq. 1 (see [17, 18]):

$$k_{sintered\ SiC} = (1 - porosity)k_{solid\ SiC} + porosity \cdot (k_{gas} + \frac{32}{3}\epsilon\sigma T^3 d_{pore}) \quad (1)$$

with  $\epsilon$  = emissivity of SiC powder,  $\sigma = 5.67 \cdot 10^{-8} \left[ \frac{W}{m^2 \cdot K^4} \right]$  (Stefan-Boltzmann constant)

The fluffy residual carbon which surrounds the source materials with evolving process time may be approximated with the physical thermal properties of a typical carbon soft felt isolation. Using this approach, temperature field calculations which match the experimental conditions quite well have been recently demonstrated (see e.g. [19]). Usually the T-field calculation (for a given heating power) in the crystal growth lab at FAU match with experimental finding with a deviation of 10 to 20°C which is an error less than 1% at the growth temperature above 2000°C.

**Note on impact of SiC source material on process yield.** In [20] it was shown that the heat conductivity of the starting SiC source material, which is strongly related to the SiC powder size distribution, has a significant influence on the temperature gradient at the crystal growth interface in a standard growth cell configuration as shown in Figs. 1 and 2. In terms of growth process yield this is a tremendous impact. In a growth run to growth run sequence, a changing SiC source heat conductivity causes varying axial temperature gradients and SiC species supersaturation at the growth interface. As reported in [20], the growth rate and even the crystal shape will vary which itself is a source for the enhanced occurrence of crystal defects lowering the growth process yield. Therefore, from the perspective of process yield it is mandatory that the SiC source properties do not vary much. It is self-explanatory that an inhomogeneous SiC source material also reduces the process yield.

## Yield Limitation during SiC PVT Bulk Growth

**Role of Heat Conductivity Carbon Isolation.** At process temperatures above 2000°C mainly carbon isolations are applied which withstand the growth conditions. At such high temperatures, degradation because of microscopic morphologic changes and aging related to Si-containing leakage of vapor from the growth cell are very common. We have designed the hotzone in a way that about 25% of the carbon isolation is replaced by new material before each growth run (Fig. 5). We rather prefer this procedure than adapting the heating power in a growth run to growth run manner, until the isolation unit is basically “consumed”.

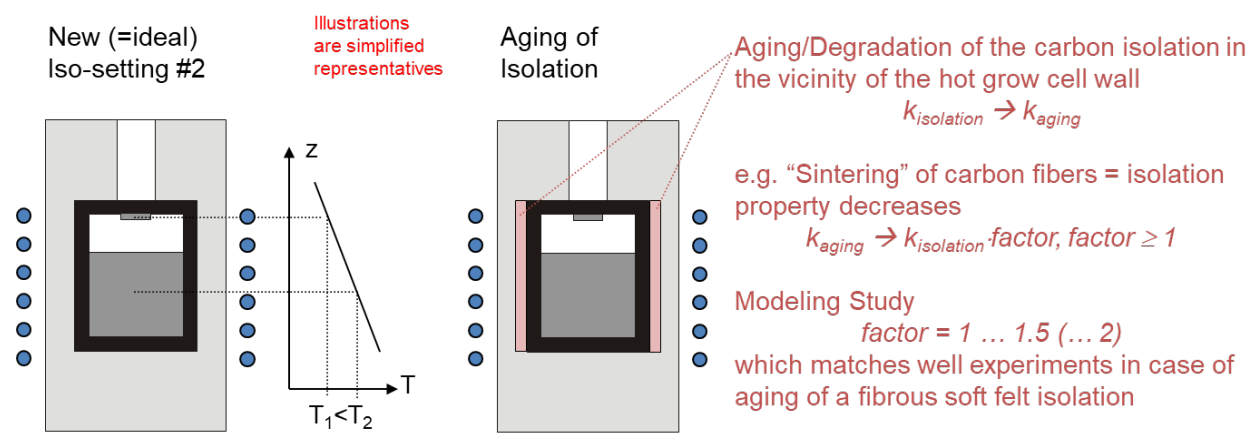


**Fig. 4.** Illustration of the areas where the carbon isolation ages significantly during a PVT growth process.

**Table 1.** Heating Power versus growth temperature (top of crucible) (basic hot-zone configuration I, cooling channel B, crucible variant #2,) of 4 nominally equal growth processes.

| Power set point [kW] | T at crucible top [°C] | Growth rate [ $\mu\text{m/h}$ ] |
|----------------------|------------------------|---------------------------------|
| 15.5 +/- 0.1         | 2020 +/- 20            | 143 +/- 4                       |

Hereby we are able to start each growth process with extremely high reproducibility using the power process control mode (see section on “Power versus temperature process control” and example presented in Table 1). Using these procedures, the T-measurement by optical pyrometers on top of the growth cell indicated a high process reproducibility. In the case of an induction heating power of 15.5 kW, we observed a constant temperature of 2020°C at the crucible top which varied only by +/-20°C (see Table 1). This value fluctuation is less than 1% which comes close to measurement precision of optical ratio pyrometers. In addition, the observed crystal growth rate of ca. 140  $\mu\text{m/h}$  (determined in the center of the boule) varied less than 3%. Both values indicate that the evolution of the SiC crystal growth process has become very reproducible with the routinely replacement of 25% of the most aged carbon isolation.

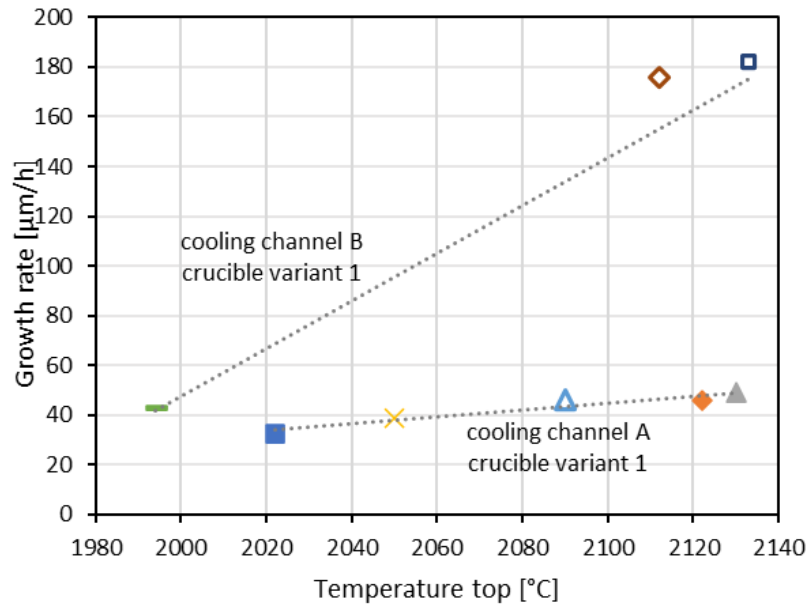


**Fig. 5.** Relation of growth rate versus Temperature at crucible top for two different cooling channels A and B (crucible variant #1, basic hotzone configuration I).

Experimentally, in several different hot-zone designs (this study and also former studies not shown here) and fixed inert-gas pressure we observed an almost linear growth rate to temperature (or heating power) relation. Since the growth rate is dependent on many thermodynamic as well as growth-kinetic phenomena, this finding represents more like a rule of practice, which proved to be valuable for the planning of new PVT growth processes. Fig. 5 depicts the temperature to growth rate evolution for two 150 mm hot-zone designs (= different cooling isolation settings A and B) of this study. The result indicates on one hand that a quite precise tuning of the SiC crystal growth rate is possible which is intended to lay around 150  $\mu\text{m/h}$ . On the other hand, the result also supports the constant power process control which enables a steady (= undisturbed) growth process (detailed discussion see in the forthcoming section on “Power versus temperature process control”).

To further elucidate the role of the carbon isolation properties and to deduce a more general understanding of the experimental results presented in Table 1 and Fig. 5, we have carried out computer simulation of the thermal field of our growth setup. The area of the carbon isolation which suffers most during a high temperature PVT process is located directly in contact with the dense graphite crucible. The hottest areas are located in the cylindric part which surround the crucible as indicated in Fig. 4 (center image).

During aging of fibrous carbon isolation, densification and a kind of sintering of the fiber is observed, which causes a local increase of the material heat conductivity. To account for this aging / degradation we adapted the temperature heat conductivity by a constant factor. As definition, an increase of the heat conductivity due to sintering of the isolation fibers by the factor 1.2 or 1.5 equals an isolation degradation by 20% or 50%, respectively. From an experimental point of view, we often observed an aging of the directly to the crucible attached fibrous isolation by  $25\% \pm 10\%$  (comparison of 11 processes with identical settings) for growth runs of ca 100 hours. The aging value will further increase for longer growth runs (or repeated growth runs with no exchange of the aged isolation parts).

Computer simulation of the temperature field of the 150 mm PVT hotzone shows that the temperature at the crucible top increases linearly with the heating power at typical growth regimes at  $T > 2000^\circ\text{C}$  (Fig. 6). Due to fact that the thermal properties of the hotzone components are nonlinear, this finding is surprising and reflects a special feature of the FAU hotzone design. Interestingly, in case of aging, this linear behavior remains, however, the temperature drops at a constant heating power due to the altered thermal isolation.

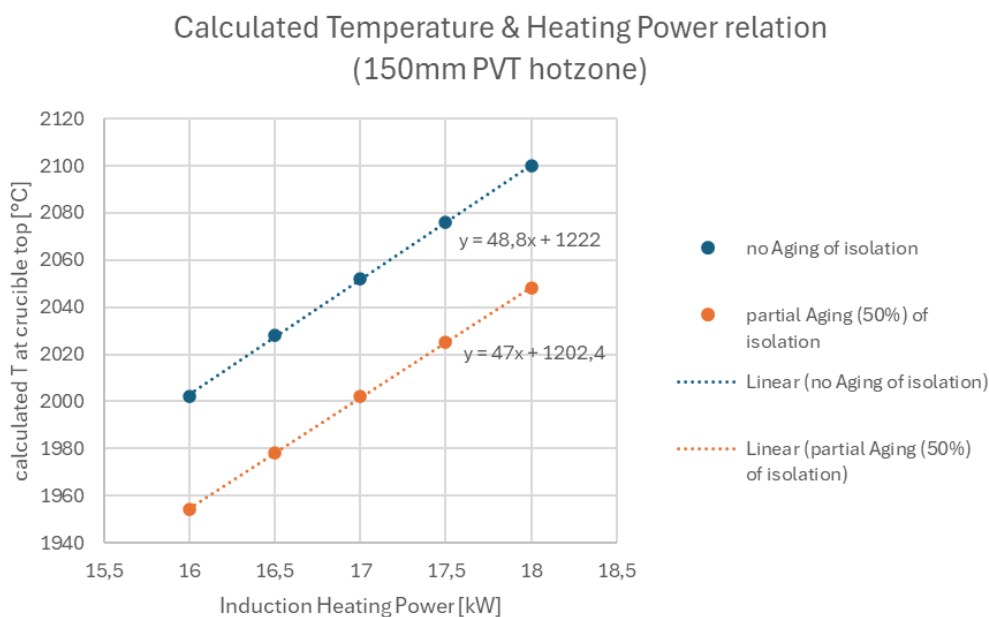


**Fig. 6.** Computer simulation of the Temperature field: Analysis of the temperature on of the growth cell as a function of the heating power for two cases of carbon isolation aging (new and aging of 50% in the vicinity of the crucible).

**Table 2.** Computer simulation of the temperature field: Impact of the heating power on the crucible top temperature, the temperature gradients and related supersaturation at the growth interface.

| <b>P coil<br/>[kW]</b> | <b>T crucible<br/>top [°C]</b> | <b>T diff crucible<br/>top-bottom<br/>[°C]</b> | <b>T radial<br/>gradient<br/>[°C/cm]</b> | <b>Supersaturation <math>\sigma</math><br/>of growth limiting<br/>species SiC<sub>2</sub></b> | <b><math>\Delta\sigma</math> compared<br/>to 16 kW<br/>heating [%]</b> |
|------------------------|--------------------------------|------------------------------------------------|------------------------------------------|-----------------------------------------------------------------------------------------------|------------------------------------------------------------------------|
| 16.0                   | 2002                           | 239                                            | 1.2                                      | 0.41                                                                                          | 0                                                                      |
| 16.1                   | 2007                           | 239                                            | 1.1                                      | 0.40                                                                                          | -0.5                                                                   |
| 16.2                   | 2012                           | 240                                            | 1.1                                      | 0.40                                                                                          | -0.9                                                                   |
| 16.3                   | 2017                           | 240                                            | 1.1                                      | 0.40                                                                                          | -1.4                                                                   |
| 16.4                   | 2022                           | 240                                            | 1.1                                      | 0.40                                                                                          | -1.8                                                                   |
| 16.5                   | 2027                           | 241                                            | 1.1                                      | 0.40                                                                                          | -2.3                                                                   |
| 16.7                   | 2037                           | 241                                            | 1.1                                      | 0.39                                                                                          | -3.2                                                                   |
| 17.0                   | 2052                           | 242                                            | 1.1                                      | 0.39                                                                                          | -4.5                                                                   |
| 17.5                   | 2076                           | 244                                            | 1.1                                      | 0.38                                                                                          | -6.5                                                                   |
| 18.0                   | 2099                           | 246                                            | 1.1                                      | 0.37                                                                                          | -8.5                                                                   |

Interestingly, during power increase (Table 2) the calculated temperature difference between crucible top and bottom as well as the radial temperature gradient at the seed remain almost constant at around 240°C and 1.1°C/cm, respectively. As expected, the supersaturation (driving force for crystallization) at the seed slightly drops. Note: The SiC growth process is carried out with low inert gas pressure (200 to 1000 Pa) which lies in the same range as the subliming SiC-related gas species Si, Si<sub>2</sub>C and SiC<sub>2</sub>. Therefore, the growth rate is only slightly diffusion limited but rather determined by the sublimation rate of the SiC powder. This coincides with the experimental finding in Fig. 5 that the growth rate increases with process temperature.

In the next step we have analyzed our modelling data with the aim to identify the necessary higher heating power to compensate the heat loss in the case of an aged isolation (plot in Fig. 7 and data set in Table 3). To maintain a constant crucible temperature, the aging of the carbon isolation can be compensated by a higher heating power. Up to an aging of 60% a linear heating power to aging relation is found. At aging values of 70% and higher a sublinear relation is found. The latter indicates that the outer, not aged isolation retains a further heat loss once the inner part is basically “consumed” (compared to the unaged outer isolation part).

**Table 3.** Computer simulation of the temperature field: Impact of aging of the carbon isolation in the vicinity of the crucible on the T-field at constant heating power.

| <b>Aging<br/>1=new<br/>1.5=50% aging<br/>2.0=100% aging</b> | <b>P coil<br/>[kW]</b> | <b>T crucible<br/>top [°C]</b> | <b>T diff crucible<br/>top-bottom [°C]</b> | <b>T radial gradient<br/>[°C/cm]</b> |
|-------------------------------------------------------------|------------------------|--------------------------------|--------------------------------------------|--------------------------------------|
| 1.0                                                         | 16.0                   | 2002                           | 239                                        | 1.2                                  |
| 1.1                                                         | 16.0                   | 1992                           | 238                                        | 1.2                                  |
| 1.2                                                         | 16.0                   | 1980                           | 238                                        | 1.2                                  |
| 1.3                                                         | 16.0                   | 1971                           | 237                                        | 1.2                                  |
| 1.5                                                         | 16.0                   | 1954                           | 237                                        | 1.2                                  |
| 1.7                                                         | 16.0                   | 1940                           | 236                                        | 1.2                                  |
| 2.0                                                         | 16.0                   | 1923                           | 235                                        | 1.2                                  |

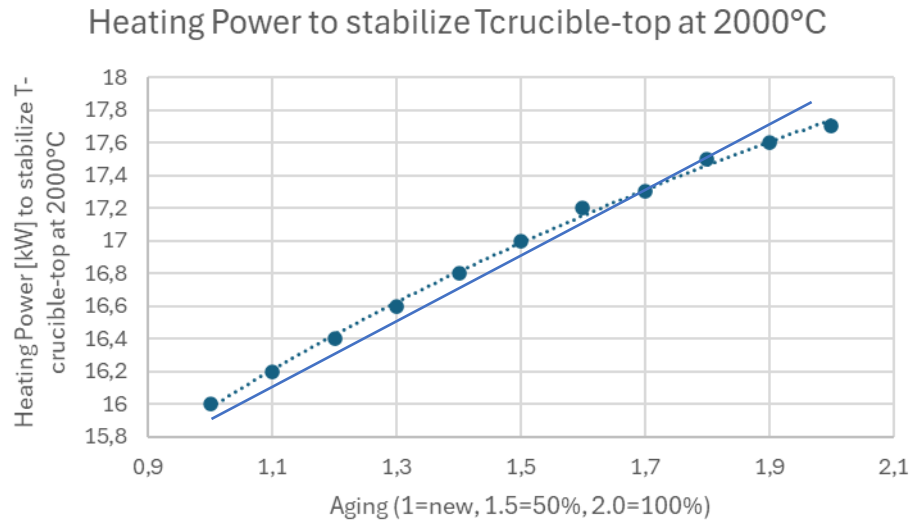


**Fig. 7.** Computer simulation of the temperature field: Compensation of the heat loss due to aging by increase of the heating power (case: constant temperature at crucible top).

**Table 4.** Computer simulation of the temperature field: Compensation of the heat loss due to aging by increase of the heating power (case: constant temperature at crucible top) and influence on temperature gradients and SiC growth conditions inside the crucible.

| Aging             | P coil<br>[kW] | T crucible<br>top [°C] | T diff<br>crucible<br>top-bottom<br>[°C] | T radial<br>gradient<br>[°C/cm] | Supersaturation<br>of growth limiting<br>SiC <sub>2</sub> species |
|-------------------|----------------|------------------------|------------------------------------------|---------------------------------|-------------------------------------------------------------------|
| 1=new             |                |                        |                                          |                                 |                                                                   |
| 1.5=50%<br>aging  |                |                        |                                          |                                 |                                                                   |
| 2.0=100%<br>aging |                |                        |                                          |                                 |                                                                   |
| 1.0               | 16.0           | 2002                   | 239                                      | 1.2                             | 0.41                                                              |
| 1.1               | 16.2           | 2001                   | 239                                      | 1.2                             | 0.41                                                              |
| 1.2               | 16.4           | 2000                   | 239                                      | 1.2                             | 0.41                                                              |
| 1.3               | 16.6           | 2000                   | 240                                      | 1.2                             | 0.41                                                              |
| 1.5               | 17.0           | 2002                   | 240                                      | 1.2                             | 0.41                                                              |
| 1.7               | 17.3           | 2001                   | 241                                      | 1.2                             | 0.41                                                              |
| 2.0               | 17.7           | 2001                   | 242                                      | 1.2                             | 0.41                                                              |

Table 3 shows a further import property of the FAU hot zone design to reach reproducible growth runs. The axial and radial temperature gradients inside the growth cell remain “untouched” by the aging of parts of the thermal isolation and heating power compensation. Again, due to the nonlinear T-dependency of the thermal carbon materials properties, one would have expected a more complex system reaction. In the case of a heating power adaptation to compensate the isolation aging related heat losses (Table 4) even a constant supersaturation at the growth front of the seed is observed. These constant values prove that the thermal management how to heat and how to maintain the outflow of heat has been resolved in the FAU hotzone in a very good manner. The latter being a prerequisite for a high crystal growth yield. From the reported finding one may conclude that the FAU hotzone is quite feasible to be used in a mainly temperature-based process control. Because of the risk of a temperature measurement error, however, we favor the mainly power controlled PVT process.

**Power versus temperature process control.** Considering a T-measurement error of optical pyrometers of at least  $\pm 10^\circ\text{C}$  at  $T > 2000^\circ\text{C}$  and potential distortions in the optical alignment of the system during the growth process, a total T-measurement error of  $10\text{--}20^\circ\text{C}$  is typical. Nevertheless, distortions in the T-measurement above  $50^\circ\text{C}$  may occasionally occur. In addition, a thermally highly isolated hot-zone (to save heating energy) exhibits long reaction intervals before a change in the heating power affects the hot-zone temperature. Therefore, it is recommended to use the temperature measurement/control as an indicator that the right T-value for a given heating power has been reached at the beginning of the growth process. Throughout the growth process a constant heating power mode is recommended for stable growth process conditions (Fig. 8). This includes a precise monitoring of the temperature of the hotzone and an optional soft feedback-loop to power control like a soft power adaption to keep the supersaturation at the growth front constant.

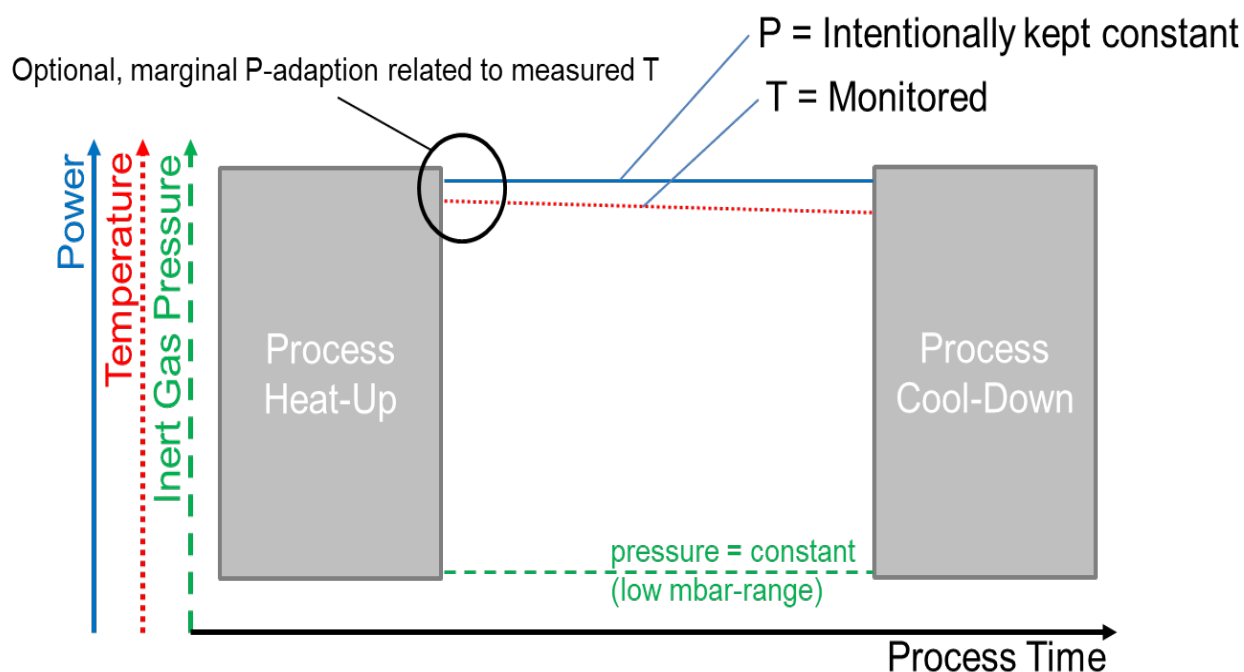


**Fig. 8.** Sketch of the suggested Power controlled PVT growth process.

**Indicators for reproducible growth conditions.** The simple dataset of heating power, temperature of the hot-zone (top and/or bottom pyrometer) and the growth rate (or final crystal height/weight at a given duration of the growth period, see Fig. 3) as used in Table 1 proved to be powerful to validate reproducible growth condition. Additional valuable data to be monitored (not discussed in this paper) are weight changes of the crucible and other hot zone components and inspection of the carbon isolation parts to identify/quantify aging.

Other indicators, like shape of the crystal cap (= growth interface), position and size of crystal facets or macroscopic morphologic features of the crystal cap are more related to hotzone design, the seed mounting/pre-preparation or the impacts of the source material which were not in the scope of this study.

## Summary

We reported on how heating isolation improves the yield during SiC crystallization using the PVT method. Systematic monitoring of the aging of the carbon isolation and partial renewal of distorted areas are crucial to maintaining stable, reproducible growth conditions. This partial material exchange procedure enables nearly complete recovery of aging carbon isolation. Therefore, the authors strongly favor this procedure over continuous usage of carbon isolation, which requires steady aging to be



compensated for by adapting the heating power from one growth run to the next. In addition to partially renewing the carbon isolation, we favor a power-controlled growth process over the temperature-controlled process. However, a soft, optional releveling of the power to maintain a constant temperature on the crucible top or bottom is believed to increase the yield of the growth process.

## Acknowledgements

This work has been partially funded by the German Science Foundation (contracts WE2107-12/2, WE 2107-15/2) and PVA Crystal Growing Systems GmbH (Wettenberg, Germany)(contract wtt-19174).

## References

- [1] P. J. Wellmann, J. Steiner, S. Strüber, M. Arzig, M. Salamon, N. Uhlmann, B. D. Nguyen, S. Sandfeld, *Diamond and Related Materials*, 109895 (2023)
- [2] P. J. Wellmann, M. Arzig, J. Ihle, M. Kollmuss, J. Steiner, M. Mauceri, D. Crippa, F. La Via, M. Salamon, N. Uhlmann, M. Roder, A. N. Danilewsky, B. D. Nguyen, S. Sandfeld, *Materials Science Forum*, 1062, 104 (2022)
- [3] P. Wellmann, M. Schöler, P. Schuh, M. Jennings, F. Li, R. Nipoti, A. Severino, R. Anzalone, F. Roccaforte, M. Zimbone, F. La Via, "Status of 3C-SiC Growth and Device Technology," in *Wide Bandgap Semiconductors for Power Electronics*, 2021, pp. 93.
- [4] J. Steiner, M. Arzig, A. Denisov, P. J. Wellmann, *Crystal Research and Technology*, 55, 2, 1900121 (2020)
- [5] M. Pons, E. Blanquet, J. M. Dedulle, I. Garcon, R. Madar, C. Bernard, *J. Electrochem. Soc.*, 143, 11, 3727 (1996)
- [6] D. Hofmann, R. Eckstein, M. Kölbl, Y. Makarov, S. G. Müller, E. Schmitt, A. Winnacker, R. Rupp, R. Stein, J. Völkl, *Journal of Crystal Growth*, 174, 669 (1997)
- [7] Y. E. Egorov, A. O. Galyukov, S. G. Gurevich, Y. N. Makarov, E. N. Mokov, M. G. Ramm, M. S. Ramm, A. D. Roenkov, A. S. Segal, Y. A. Vodakov, A. N. Vorob'ev, A. I. Zhmakin, *Mat.Sci.Forum*, 264-268, 61 (1998)
- [8] M. Selder, L. Kadinski, Y. Makarov, F. Durst, P. Wellmann, T. Straubinger, D. Hofmann, S. Karpov, M. Ramm, *Journal of Crystal Growth*, 211, 333 (2000)
- [9] P. J. Wellmann, M. Pons, *Journal of Crystal Growth*, 303, 337 (2007)
- [10] R. Ma, H. Zhang, V. Prasad, M. Dudley, *Crystal Growth & Design*, 2, 3, 213 (2002)
- [11] P. J. Wellmann, M. Bickermann, D. Hofmann, L. Kadinski, M. Selder, T. L. Straubinger, A. Winnacker, *Journal of Crystal Growth*, 216, 263 (2000)
- [12] P. Wellmann, G. Neubauer, L. Fahlbusch, M. Salamon, N. Uhlmann, *Crystal Research and Technology*, 50, 1, 2 (2015)
- [13] M. Arzig, M. Salamon, N. Uhlmann, P. J. Wellmann, *Advanced Engineering Materials*, ja, 1900778 (2019)
- [14] M. Schöler, P. Schuh, J. Steiner, P. J. Wellmann, *Materials Science Forum*, 963, 157 (2019)
- [15] J. Ihle, P. J. Wellmann, *Crystal Research and Technology*, n/a, n/a, 2400080 (2024)
- [16] M. Arzig, J. Steiner, M. Salamon, N. Uhlmann, P. J. Wellmann, *Materials*, 12, 16, 2591 (2019)

- [17] A. L. Loeb, *Journal of the American Ceramic Society*, 37, 2, 96 (1954)
- [18] R.-H. Ma, Q.-S. Chen, H. Zhang, V. Prasad, C. M. Balkas, N. K. Yushin, *Journal of Crystal Growth*, 211, 352 (2000)
- [19] J. Schultheiß, J. Ihle, S. Nanot, S. Bonanomi, D. Munoz, R. Hammer, P. Wellmann, *Solid State Phenomena*, 362, 65 (2024)
- [20] M. Arzig, M. Salamon, N. Uhlmann, B. A. Johansen, P. J. Wellmann, *Materials Science Forum*, 924, 245 (2018)